Optical Engineering

SPIEDigitalLibrary.org/oe

# 193-nm-laser-induced spectral shift in HR coated mirrors

Byungil Cho
J. Earl Rudisill
Edward Danielewicz

SPIE

# 193-nm-laser-induced spectral shift in HR coated mirrors

**Byungil Cho**
**J. Earl Rudisill**
**Edward Danielewicz**
Newport Corporation
1791 Deere Avenue
Irvine, California 92606
E-mail: byungil.cho@newport.com

**Abstract.** High-reflectance mirrors, fabricated by use of fluoride coating materials, were irradiated for extended periods by a 193-nm kilohertz repetitive laser source. This irradiation promoted a spectral shift in the reflectance band towards shorter wavelengths. In efforts to determine the mechanism for the observed spectral shifts, various models were investigated by employing such techniques as spectrophotometry, surface profile interferometry, coating design simulation, and x-ray diffraction. The result of the investigation indicates that layers near the top surface of the coating structure underwent densification, which resulted in the observed spectral shift.  [DOI: 10.1117/1.OE.51.12.121804]

Subject terms: 193-nm; laser induced; spectral shift; fluoride; high-reflectance mirror; densification; compaction; crystallization.

Paper 120366SSP received Mar. 13, 2012; revised manuscript received May 30, 2012; accepted for publication Jun. 6, 2012; published online Jul. 10, 2012.

## 1 Introduction

It has been known that point defects such as vacancies and micropores are formed during thin film deposition. Apparently, thin film condensation is thus accompanied by the incorporation of large nonequilibrium concentrations of point defects. This can cause lower film density than the bulk density. The gradient in film density is attributed to several causes such as high crystalline disorder, formation of oxides, greater trapping of vacancies and holes, pore production by gas incorporation, and special growth modes that dominate the early stage of film formation.[1]

There is a continuing technological need to increase the useful life of optical coatings for deep ultraviolet (DUV) applications. The coating material selection is important in providing high laser-induced damage thresholds. Dielectric fluorides are excellent optical coating materials for 193-nm application due to their high transparency and low absorption.[2,3] However, evaporated fluoride films do contain the defects mentioned above, and, if heated, thermally activated atomic and/or molecular diffusion may readily take place. This reasoning follows from the knowledge that vacancies and micropores are known to play a key role in fostering diffusion in solid state materials.

It is thus likely that heating in the dielectric coating layers of a high-reflectance (HR) mirror will modify thin film microstructures, which in turn will affect the stress, optical, and mechanical properties of the total coating stack. It would be interesting to understand the behavior of HR coatings that absorb thermal energy through irradiation of laser photons.

In this paper an investigation of 193-nm laser irradiation of dielectric HR coatings was undertaken. This study included examination of surface morphology utilizing a surface profile interferometer, simulation of optical performance employing coating design software, and analysis of material crystal structures by x-ray diffractometry. Three models are presented for understanding the observed spectral reflectance.

0091-3286/2012/$25.00 © 2012 SPIE

## 2 Approach

All dielectric HR (193-nm) mirrors consisting of $AlF_3/LaF_3/Al_2O_3$ thin film layers were deposited on DUV-grade fused silica. The dielectric oxide films were necessary because the previous work had shown that their intrinsic compressive stress could compensate for the large tensile stress of the fluoride layers and thus minimize the overall stress of the multilayer coating.[4] Otherwise, the highly tensile stress in the films lead to increase scattering losses through stress reduction via material cracking, crazing, or delamination. The HR mirror coatings were deposited by thermal boat evaporation for the fluorides and by e-beam evaporation for the oxide layers. The coating chamber was initially pumped by an oil-free, dry roughing pump and followed by cryo-pumping to attain high vacuum base pressures in the low $10^{-8}$ Torr range. During deposition the thickness control for each layer was determined by optical monitoring, and the deposition rate was controlled by quartz crystal monitors.

These HR mirrors were then irradiated by a 193-nm kilohertz repetitive laser source for an extended time. The reflectance of as-coated and postirradiated mirrors was measured by a DUV spectrophotometer (Acton Research, model CAMS-507). The surface morphology was analyzed with an interferometer (ZYGO, model GPI XP), and x-ray diffraction patterns were obtained by a Siemens D500 diffractometer. The diffractometer operated at 40 kV and 30 mA with a CuK$\alpha$ target. The start incident angle and end incident angle were 20 and 70 deg, respectively. The step size was 0.02 deg.

## 3 Results and Discussion

### 3.1 *Reflectance*

The reflectance of as-coated and postirradiated mirrors was measured in the wavelength range of 170 to 210 nm with the spectrophotometer. A footprint of the laser beam profile was observed on postirradiated samples. The reflectance of these 193-nm irradiated coatings was then measured at a variety of points ($x = 0$, 5 and 15 mm) where $x$ is the distance between

the footprint center and the measured spot on the sample surface (Fig. 1). The data show that the reflectance curves of the postirradiated coatings are shifted towards shorter wavelengths. The effect can be observed with fluence as low as 1 $mJ/cm^2$. On the contrary, in a previous paper[5] the position of the minimum transmission (i.e., maximum reflectance) was shifted by 2 nm to longer wavelengths after an HR coating ($Al_2O_3/SiO_2$) was irradiated by a 308-nm laser.

The data in Fig. 1 also shows the distance dependence of the spectral reflectance shift. That is, they are shifted, when measured at the 50% reflectance of each curve, by 4.3, 1, and 0.5 nm. However, these shifts are not linear, with more shifting on the longer than on the shorter wavelength sides of the reflectance curve profile.

### 3.2 *Surface Morphologies*

The surface morphology of each postirradiated coating was then examined with an interferometer. The surface image in the upper left corner of Fig. 2 shows the area affected by the laser beam. The oblique plot image in the upper right corner and the surface profile data at the lower left in Fig. 2 reveal a crater. Its diameter was approximately 6 mm and maximum depth is ~90 nm, but the average depth was estimated to be 30 nm. Previous studies have demonstrated that the craters were formed when the optics were irradiated by a laser with high fluence and short pulse duration.[6] The laser-induced damages were reported to be revealed by melting, fracture, evaporation, and ablation of the surface.[7–9] In this paper, the formation of the crater is mainly attributed to the densification of thin film layers rather than to loss of film layer material. This is based on the assumption that the surface of the HR coating was being exposed to the absorption of heat, as will be discussed later.

The crater was found to be surrounded with wings and a bulge, which were presumably caused by thermoelastic expansion[10] due to thermal diffusion away from the hot central region. At lower laser fluences, a much weaker and broader bulge appears on a slower time scale.[11] The height of the low bumps in Fig. 2 was found to be $10 \sim 20$ nm.

Two models, A and B, are now presented for further understanding of the mechanism for the observed 193-nm laser-induced spectral shift of HR-coated mirrors. All models were limited to only the spectral shift (4.3 nm) that was measured at $x = 0$ mm.

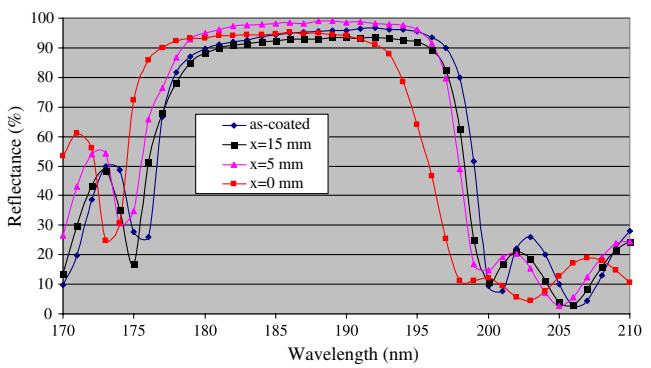


**Fig. 1** The measured reflectance of as-coated HR coating and three spots at $x = 0$, 5, and 15 mm measured after irradiation by the 193-nm laser for an extended time.

#### 3.2.1 *Model A*

In model A it is assumed that the loss of a few top layers is the cause of the spectral shift. The material loss is assumed to be due to ablation. The physical thickness of the top layers was removed from the initial coating design, and a theoretical calculation of the reflectance curve was obtained by using a commercial thin film coating design software. The modified reflectance is plotted (Fig. 3) in the wavelength range of 174 to 214 nm. For direct comparison the reflectance plot of the initial coating design is also shown in Fig. 3. The reflectance curve with loss of the top layer is broadened nearly evenly in both shorter and longer wavelengths instead of shifting to the shorter wavelengths as is observed for the postirradiated coatings. Therefore, model A could not explain the actual curve shift.

#### 3.2.2 *Model B*

The evaporated films contain point defects such as vacancies and micropores as mentioned earlier. It is known that thermally activated diffusion is facilitated by the presence of point defects in the solid state film.[12] Compaction is likely to occur by the thermally activated diffusion process during laser irradiation. The activation energy for diffusion is provided as the laser beam irradiation generates heat through absorption in the thin film coating layers. A schematic of the compaction in film layers is shown in Fig. 4. The vacancies or micropores are filled with atoms or molecules to reduce surface energy during the compaction process. This is because the driving force is to reduce free surface energy from the defects in the film layers and is accomplished through compaction. The film material tries to reach its true equilibrium configuration, which has thermodynamically lower energy and higher density.[13]

The change in material density modifies the microstructure, which affects the stress, mechanical, and optical properties of the thin film coatings. Previously, it was found that high-intensity laser interaction with an amorphous $SiO_2$ film increased its density and refractive index.[14] Densification of fused silica was also widely reported in previous studies.[15–17] However, this paper is concentrated on the densification of the optical coatings. The substrate effect on the absorption was neglected due to the low transmission through the HR coatings, lower than 1%.[18]

The diffusion coefficient $D$ increases exponentially with the temperature as shown in Eq. (1).

$$D = D_0 \exp(-Q/\mathrm{RT}), \tag{1}$$

where $D$ is the diffusion coefficient ($cm^2/s$), $D_0$ is a constant ($cm^2/s$), $Q$ is activation energy (kcal/mole), $T$ is absolute temperature (K), and $R$ is the gas constant (1.98 cal/K · mole).

The relationship of diffusion distance $X$ with the diffusion coefficient and time $t$ is shown in Eq. (2). The diffusion distance increases with the diffusion coefficient and time.

$$X = \sqrt{Dt}. \tag{2}$$

The higher temperature, the greater is the layer compaction that occurs at a fixed time since the diffusion distance increases with the diffusion coefficient. The distance dependence of the laser-induced curve shift observed in Fig. 1 was

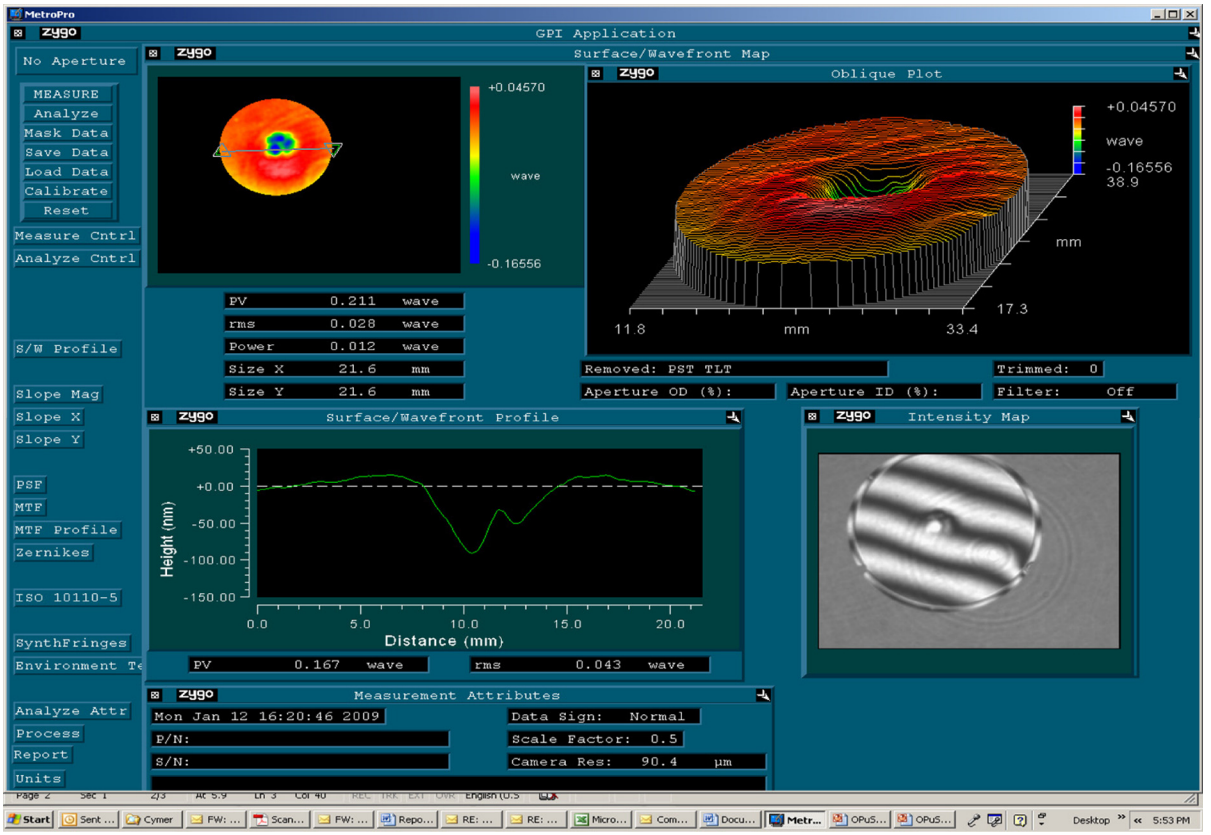


**Fig. 2** Surface morphology of HR coating measured by an interferometer after the HR coating was irradiated with a 193-nm laser for an extended time.

attributed to Gaussian distribution of the temperature on the HR coating surface.

### 3.3 *Case 1*

It was reported that the film density and the refractive index increased as a result of the film densification.[16,17] In case 1, three possible assumptions were made. In assumption 1, of three materials only $AlF_3$ experienced 5% reduction in the physical thickness and 5% increase in the refractive index, while the other two materials remained unchanged.

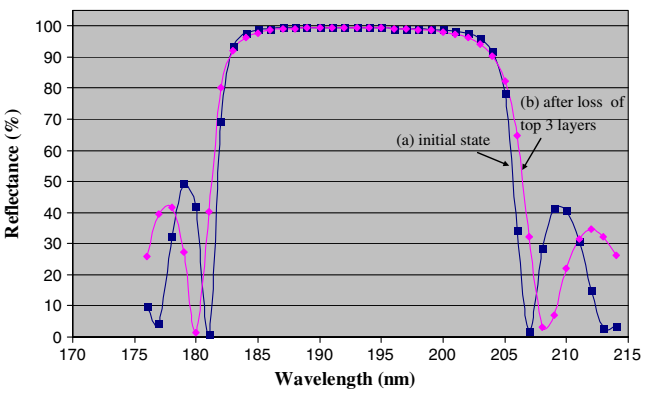


**Fig. 3** (a) Initial state, and (b) after the top three layers were lost by the irradiation of the 193-nm laser.

Likewise, in assumptions 2 and 3, only $LaF_3$ and $Al_2O_3$ had the same amount of modifications, respectively. The reflectance was calculated in the wavelength range of 170 to 214 nm based on the modified stack formula by using the coating design software and was plotted in Fig. 5. The reflectance of the initial coating design without compaction was also plotted in Fig. 5.

In assumption 1 for $AlF_3$, the reflectance curve was narrowed excessively (i.e., ~30%) compared to Fig. 1 although it was shifted toward the shorter wavelengths. In assumption 2 for $LaF_3$, the reflectance curve was broadened 34.7% and was shifted more in the shorter wavelengths than in the longer wavelengths. However, in contrast to assumption 2, the actual reflectance curve was shifted more in the longer wavelengths than in the shorter wavelengths. In assumption 3 for oxide, the reflectance spectrum simply was broadened 43.5% instead of shifting. None of three cases above were close to the actual spectral shift of Fig. 1.

### 3.4 *Case 2*

Case 2 considered two dozen different assumptions that involved a numeric change in the physical thickness and the refractive index of three materials. Among them, in Fig. 6, the best match with the actual data ($x = 0$ mm) was found when the following two assumptions were made: (1) In all $AlF_3$ layers, the physical thickness decreased by 3.5% and the index increased by 1.5%. There are more free spaces such as vacancies or micropores in the $AlF_3$ film layers than in $LaF_3$ and $Al_2O_3$ film layers since $AlF_3$ layers

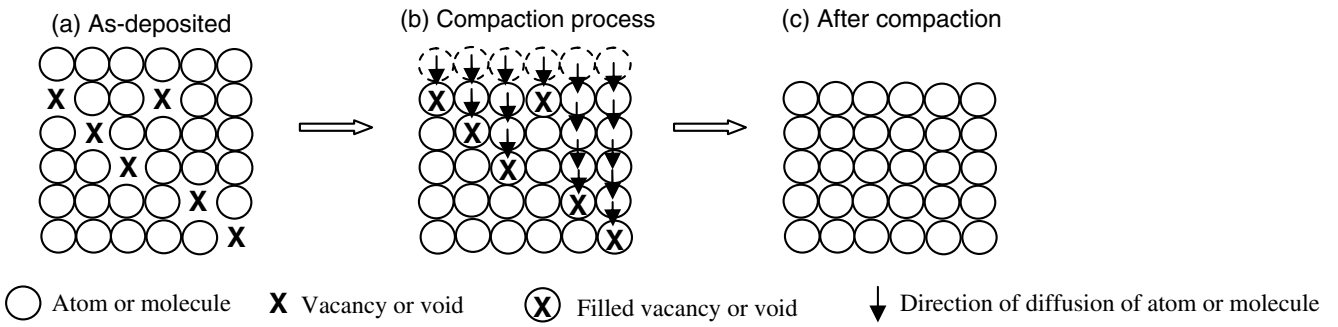


**Fig. 4** Schematic compaction process controlled by thermally activated diffusion.

have a relatively loosely bound structure. The defects in the solid state materials and the low melting point of the film material facilitate thermally activated diffusion, as mentioned earlier. Therefore, it is likely that compaction of all $AlF_3$ layers occurred throughout the whole stack of film. (2) The compaction of $LaF_3$ and oxide films occurred only in the top nine layers of the surface accompanying 3.5% decrease in the physical thickness and 1% increase in the refractive index. The x-ray diffraction test results suggested that the compaction and partial crystallization occurred in $AlF_3$ layers, as will be discussed later.

### 3.5 *Crystal Structures*

For structural studies of an irradiated HR coated mirror, the identification of any crystalline state at $x = 0$, 5, and 15 mm was made with an x-ray diffractometer. The x-ray diffraction patterns in Fig. 7 show that $LaF_3$ films were crystalline and $AlF_3$ films were amorphous at $x = 15$ mm, respectively, as previously reported.[3] $LaF_3$ films were confirmed to have hexagonal structure. The oxide films were amorphous. It is interesting that a low degree of compaction was so sensitively detected by the reflectance curve shift (0.5 nm) in Fig. 1.

The crystalline state of the three materials did not change at $x = 5$ mm in Fig. 8 in comparison with that at $x = 15$ mm in Fig. 7. However, the compaction actually progressed further, as the data showed that the reflectance curve shift increased from 0.5 to 1 nm as $x$ decreased from 15 to 5 mm in Fig. 1.

The data of Fig. 9 showed that a noticeable onset of crystallization of amorphous $AlF_3$ films occurred as $x$ moved to the hottest region ($x = 0$ mm) of the HR coating while the crystalline states of $LaF_3$ and $Al_2O_3$ remained unchanged. The low peak intensity of $AlF_3$ in the x-ray diffraction patterns indicated that the amorphous film layers partially crystallized due to optical absorption heating. The first (102), second (200), and third (103) peaks were due to the crystalline hexagonal phase $AlF_3$.

The crystallization that occurs by thermally activated atomic diffusion is similar to the compaction. The compaction at $x = 0$, 5, and 15 mm was clearly noticed by the spectral shift as observed in Fig. 1 although it was detected only at $x = 0$ mm by x-ray diffraction. The compaction likely first occurs in a form of short-range atomic rearrangements, and then the crystallization takes place if it further progresses into the stage accompanying long-range atomic movements. There would be more decrease in free volume in crystallization than in compaction. It has been known that the free volume in amorphous

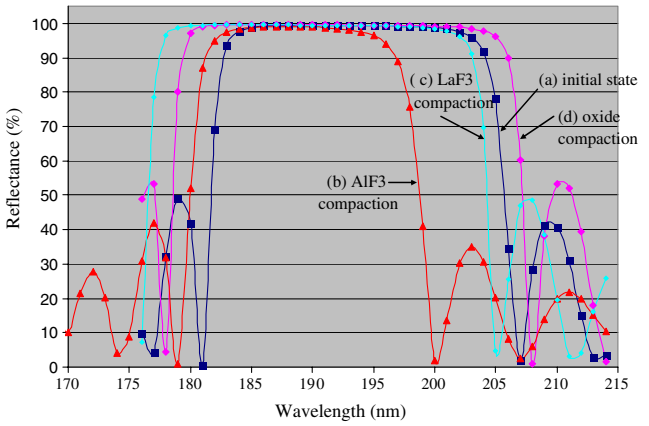


**Fig. 5** (a) Initial state, and three assumptions: (b) assumption 1, compaction of only $AlF_3$; (c) assumption 2, compaction of only $LaF_3$; and (d) assumption 3, compaction of only $Al_2O_3$. In each of the three assumptions, only one of three materials such as $AlF_3$, $LaF_3$, and $Al_2O_3$ experienced 5% reduction in the physical thickness and 5% increase in the refractive index due to compaction.

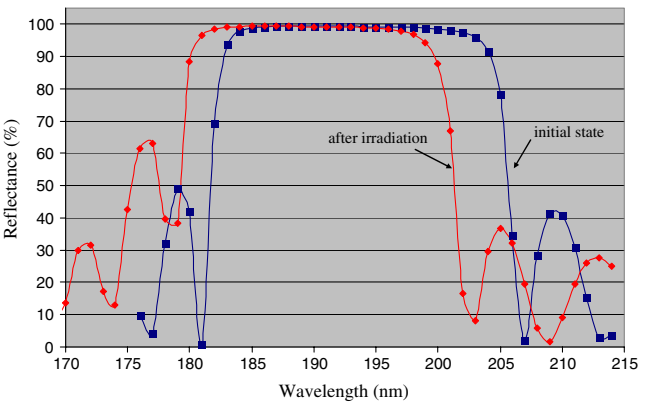


**Fig. 6** Initial state, and two assumptions: the compaction occurred in all $AlF_3$ films throughout the whole layer stack. However, $LaF_3$ and $Al_2O_3$ within the top nine layers of the surface experienced the compaction.

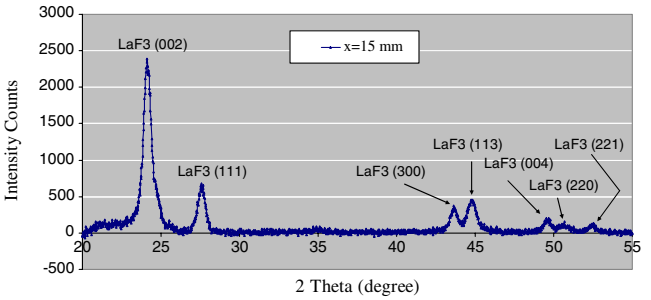


**Fig. 7** X-ray diffraction patterns of an irradiated HR mirror coating at $x = 15$ mm.

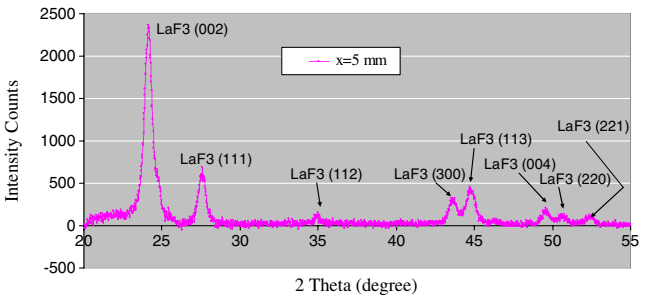


**Fig. 8** X-ray diffraction patterns of an irradiated HR mirror coating at $x = 5$ mm.

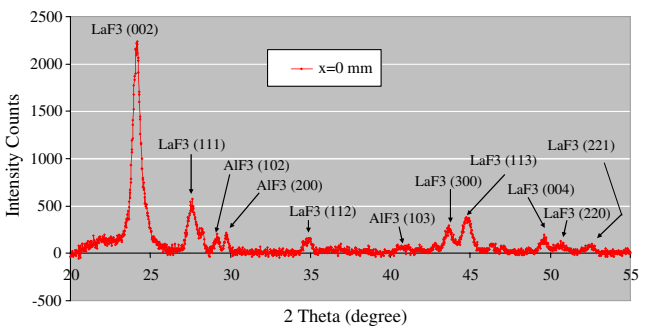


**Fig. 9** X-ray diffraction patterns of an irradiated HR mirror coating at $x = 0$ mm.

structures decreases and the film density increases during crystallization.[1] The most spectral shift (4.3 nm) at $x = 0$ mm seems to be due to the partial crystallization of $AlF_3$ in addition to the compaction.

## 4 Summary

The spectral reflectance curves were shifted to shorter wavelengths as dielectric coated HR mirrors were irradiated by a low-fluence 193-nm laser for an extended period of time. The curve shifted more towards shorter wavelengths as the measurement spot in the laser footprint on the mirror surface approached the center ($x = 0$ mm). This spot was relatively hottest due to the thermal distribution from heating of absorbed laser radiation. The observed reflectance curve shift and its dependence on distance from the center of the beam footprint and other measured spots were attributed to thermally activated diffusion in thin film layers of $AlF_3$, $LaF_3$, and $Al_2O_3$.

A crater of ~6 mm diameter and ~30 nm average depth was observed in the coating surface with an interferometer. A compaction resulted in a decrease in physical thickness and an increase in refractive index. In modeling, the best match of theoretical shifted reflectance curves with actual shifted curve data was found when all $AlF_3$ layers in the coating film stack were compacted, while the other two materials were densified only in the top nine surface layers. The greatest spectral shift at $x = 0$ mm (the center of the laser footprint) was attributed to the compaction and the partial crystallization of $AlF_3$, as observed in x-ray diffraction patterns.

## 5 Conclusions

Through extensive testing and modeling it was proven that the observed spectral reflectance shift from laser irradiation is caused by compaction of selected coating layers. Surprisingly, this laser-induced "damage" from compaction can be beneficial to coating performance at 193-nm.

### *Acknowledgments*

The authors give heartfelt gratitude to Mike Collin of Newport Corporation for his assistance in the preparation and deposition of the optical coatings. They also would like to thank Gene Dempsey for his interferometer measurement.

### *References*

1. M. Ohring, *The Materials Science of Thin Films*, pp. 232–234, Academic Press, New York (1992).
2. J. E. Rudsill, "Design/deposition process tradeoffs for high-performance optical coatings in the DUV spectral region," *Proc. SPIE* **5273**, 30–40 (2003).
3. M. L. Scott et al., "A review of UV coating material properties," *Damage in Laser Materials 1983*, Spec. Pub. 688, U.S. National Bureau of Standards (1985).
4. J. E. Rudsill, A. Duparre, and S. Schröder, "Determination of scattering losses in ArF* excimer laser all-dielectric mirrors for 193 nm microlithography application," *Proc. SPIE* **5647**, 9–22 (2005).
5. K. Mann, B. Granitza, and E. Eva, "Multiple-pulse damage thresholds of optical components for excimer lasers," *Proc. SPIE* **2966**, 496–504 (1977).
6. G. Demos et al., "Mechanism to explain damage growth in optical materials," *Proc. SPIE* **4347**, 277–284 (2001).
7. K. Awazu, "Ablation of amorphous $SiO_2$ using ArF excimer laser," *Proc. SPIE* **4347**, 169–176 (2001).
8. Y. Zhao et al., "Single-shot and multishot induced damage of $HfO_2/SiO_2$ multilayer at YAG third harmonic," *Proc. SPIE* **5273**, 23–29 (2004).
9. A. M. Rubenchik and M. D. Feit, "Initiation, growth and mitigation of UV laser induced damage in fused silica," *Proc. SPIE* **4679**, 79–95 (2002).
10. B. C. Li, S. Martin, and E. Welsch, "Thermoelastic influence of substrate on damage threshold of ultraviolet dielectric coatings," *Proc. SPIE* **3902**, 145–153 (2000).
11. S. R. Greenfield, J. L. Casson, and A. C. Koskelo, "Nanosecond intermediate studies of surface deformation induced by laser irradiation," *Proc. SPIE* **3902**, 108–117 (2000).
12. C. R. Barret, W. D. Nix, and A. S. Tetelman, *The Principles of Engineering Materials*, pp. 150–160, Prentice-Hall, New Jersey (1973).
13. G. Gallatin, *Mechanism of Laser Induced Compaction*, SVG Lithography, Wilton, CT, arXiv:mtrl-th/9506003 (8 June 1995).
14. C. Fiori and R. A. B. Devine, "The influence of high intensity laser irradiation on amorphous $SiO_2$ film," *Mater. Res. Soc. Symp. Proc.* **61**, 187–195 (1985).
15. R. Schenker et al., "UV damage properties of various fused silica materials," *Proc. SPIE* **2428**, 458–468 (1994).

16. V. Liberman et al., "Eximer-laser-induced densification of fused silica: laser-fluence and material-grade effects on the saling law," *J. Non-Cryt. Solids* **244**(2), 159–171 (1999).
17. A. Silins, "Defect generation in fused silica under high intensity laser interaction," *Proc. SPIE* **4347**, 207–211 (2001).
18. S. Martin, S. Bock, and E. Welsch, "Optical measurement of UV absorption in dielectric coatings," *Proc. SPIE* **4347**, 93–101 (2001).

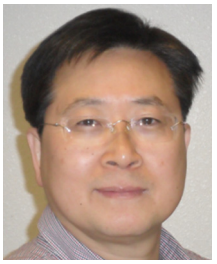

**Byungil Cho** is a senior thin film scientist at Newport Corporation, Irvine, California. He has experience in development of optical thin films with high laser-induced damage thresholds, coating design, and coating process optimization for the high power laser applications. He received BS and MS degrees from Yonsei University, Seoul, Korea and received a PhD from the University of Texas at Austin in 1994.

**J. Earl Rudisill** is a consultant in optical coating technology at Newport Corporation, Irvine, California. His experience includes design, deposition, and metrology of optical coatings, especially for high power lasers. This includes the IR ($CO_2$, CO), MIR chemical (HF, DF, OI), and DUV excimer (KF and AF) lasers. His academic background in physics includes a BS degree from the University of Maryland, and MS and PhD degrees from the University of Southern California.

**Edward Danielewicz** is a senior manager of thin film technology at Newport Corporation, Irvine, California. He has experience in all aspects of producing and testing optics for high power lasers from the IR to the DUV spectral regions. He received a BSEE from the University of Pennsylvania, and MS and PhD degrees from the University of Illinois at Champagne-Urbana.